

Leaching of Al-Based Polygrain Quasicrystalline and Related Crystalline Surfaces

T.P. YADAV^{a,*}, S.S. MISHRA^a, S.K. PANDEY^a, D. SINGH^a, M. LOWE^b, R. TAMURA^c,
N.K. MUKHOPADHYAY^d, O.N. SRIVASTAVA^a, R. MCGRATH^b, AND H.R. SHARMA^b

^aHydrogen Energy Centre, Department of Physics (Centre of Advance Studies),

^bSurface Science Research Centre and Department of Physics, The University of Liverpool, Liverpool, L69 3BX, UK

^cDepartment of Materials Science and Technology, Tokyo University of Science, Noda 278-8510, Japan

^dDepartment of Metallurgical Engineering, Indian Institute of Technology,
Banaras Hindu University, Varanasi, 221005, India

In the present investigation, we have studied leaching on polygrain Al-based quasicrystalline (*i*-Al₆₃Cu₂₅Fe₁₂) as well as crystalline (*B2* phase; Al₅₅Cu₃₀Fe₁₅) alloy surfaces using a 10 mole NaOH solution. The surface was leached at varying times from 30 min to 8 h and subsequently characterized by X-ray diffraction, scanning electron microscopy, transmission electron microscopy and energy dispersive X-ray analysis. Leaching of the samples for 30 min generated a homogeneous layer. However further leaching for 1–8 h yielded nano-size particles on the surface. Spherical microstructure has been observed on the Al–Cu–Fe crystalline surface whereas on the quasicrystalline surface a petal-like microstructure appeared. The implications of the evolution of different microstructures in the context of structure, stability and activity are discussed. The results are compared with the microstructure of leached polygrained samples containing a mixture of different surface orientations.

DOI: [10.12693/APhysPolA.126.629](https://doi.org/10.12693/APhysPolA.126.629)

PACS: 61.44.Br; 81.16.Hc; 61.66.Dk; 68.37.Hk

1. Introduction

The discovery of a quasicrystal (QC) in a rapidly-quenched Al–Mn alloy unveiled the existence of a completely different state of ordered solids [1]. After intensive investigations on their physical and mechanical properties, much interest nowadays is focused on finding practical applications for these materials [2–3]. Although, quasicrystalline materials are extremely brittle at room temperature [4], numerous studies have been undertaken to discover useful properties for their potential applications [5–8]. It is known that quasicrystals have some favorable properties, such as low adhesion behavior, high hardness, low friction coefficient, high wear resistance, low thermal conductivity and a compatible thermal expansion coefficient, indicating that these materials have potential for use in manufacturing technology [9]. One of the potential fields of the application of quasicrystalline materials is catalysis [10–13]. Since quasicrystals are equilibrium phases and are stable up to high temperature, they have the potential to be used as a catalyst at high temperature [14]. A powder of the thermally stable icosahedral (*i*) Al–Cu–Fe quasicrystal leached with NaOH aqueous solutions shows excellent activity for steam reforming of methanol [15–17]. The leaching treatments yielded Cu and Fe nanoparticles on top of the quasicrystalline surface. These nanoparticles

are believed to be responsible for catalytic behaviour. The dispersed Fe species in the homogeneous leached layer enhances the catalytic activity and suppresses the aggregation of Cu and is predominantly controlled by the dissolution rate of Al upon leaching [18]. The catalytic behavior of QC and related crystalline materials has been compared. QC catalyst has a higher catalytic activity and durability than the related crystalline catalysts [18]. Recently, the excellent performance of the QC catalyst has been described in terms of a composite structure with fine Cu nanoparticles dispersed in a (Fe,Al)₃O₄ matrix which was generated by a leaching treatment and calcination at 600 °C in air [19]. In this case, the Cu_xFe_{3-x-y}Al_yO₄ spinel structure decomposed into a composite structure with fine Cu nanoparticles dispersed in a (Fe,Al)₃O₄ matrix [20]. Recently, we have performed the leaching experiment on the well-orientated single grain fivefold (*i*)-Al–Cu–Fe and tenfold (*d*)-Al–Ni–Co quasicrystalline surface [21]. The role played by the supporting quasicrystal and the dispersed metal Cu/ Fe nanoparticle ratio in the catalytic activity is not yet fully understood and the optimization of the catalytic activity is currently limited to heuristic approaches.

In the present work, we have investigated the leaching effect on two alloys: polygrain (*i*)-Al₆₃Cu₂₅Fe₁₂ and crystalline (*B2*)-Al₅₅Cu₃₀Fe₁₅.

2. Experimental details

2.1. Synthesis

Alloys of composition Al₆₃Cu₂₅Fe₁₂, and Al₅₅Cu₃₀Fe₁₅ were prepared by melting high purity Al, Cu and Fe

*corresponding author; e-mail: yadavtp@gmail.com

(Al = 99.96%, Cu = 99.98%, Fe = 99.99%) metals in an induction furnace, in the presence of a dry argon atmosphere. The ingots formed were re-melted four times to ensure better homogeneity. The samples were cleaned by mechanical polishing using Al_2O_3 powder of $1\ \mu\text{m}$ size and subsequently washed in an ultrasonic bath with methanol for 15 min. The leaching of the surfaces of the (i)- $\text{Al}_{63}\text{Cu}_{25}\text{Fe}_{12}$ and (B2)- $\text{Al}_{55}\text{Cu}_{30}\text{Fe}_{15}$ alloys was done by using a 10 mol concentration of NaOH aqueous solution. NaOH drops were placed on the clean QC and B2 alloy surfaces by burette for 0.5–8 h at room temperature. The NaOH leached surfaces were thoroughly washed 4–5 times with methanol and distilled water in an ultrasonic bath until no trace of alkali was detected. This was confirmed through preliminary energy dispersive X-ray analysis. After each leaching experiment and subsequent characterization, the samples were re-prepared for each leaching experiments.

2.2. Characterizations

The as-grown (i)- $\text{Al}_{63}\text{Cu}_{25}\text{Fe}_{12}$ and (B2)- $\text{Al}_{55}\text{Cu}_{30}\text{Fe}_{15}$ alloys, before and after leaching, were characterized by powder X-ray diffraction (XRD) employing $\text{CuK}\alpha$ radiation ($\lambda = 1.5402\ \text{\AA}$) using X'Pert PRO (PANalytical). The characterization of the entire leached surface was done by using scanning electron microscope (SEM) FEI-QUANTA-200. Transmission electron microscopy (TEM) using FEI-TECNAI 20G² was used for microstructural and structural characterization with an operating voltage at 200 kV. Energy-dispersive X-ray analysis (EDX) attached with FEI-TECNAI 20G² electron microscope was employed for the compositional analysis.

3. Results and discussion

The first assessment of the effects of leaching on (i)- $\text{Al}_{63}\text{Cu}_{25}\text{Fe}_{12}$ and (B2)- $\text{Al}_{55}\text{Cu}_{30}\text{Fe}_{15}$ alloy surfaces was undertaken using SEM. Figure 1 shows SEM images of the leached surfaces of (i)- $\text{Al}_{63}\text{Cu}_{25}\text{Fe}_{12}$ and (B2)- $\text{Al}_{55}\text{Cu}_{30}\text{Fe}_{15}$ alloys at different leaching times. In the case of (i)- $\text{Al}_{63}\text{Cu}_{25}\text{Fe}_{12}$ surface, after 1 h the surface has been leached in depth (Fig. 1a) near the grain boundary and outlining the columnar structure which results in the formation of sub-micrometer porosity on the surface. For (B2)- $\text{Al}_{55}\text{Cu}_{30}\text{Fe}_{15}$ the surface looks more porous (Fig. 1(e)). For further leaching times i.e. 2, 4, and 8 h, tiny particles are observed on both (i)- $\text{Al}_{63}\text{Cu}_{25}\text{Fe}_{12}$ and (B2)- $\text{Al}_{55}\text{Cu}_{30}\text{Fe}_{15}$ which was confirmed using high magnification SEM investigation (1b-d & f-h). It was found that the density of the particles is much higher on the QC leached surface. The corresponding EDX spectra show that these particles are composed of Cu and Fe. These particles are in good shape when leached for 2 and 4 h; while further leaching for 8 h, the particles become rougher. The appearance of such roughness may be due to the reaction of these particles with NaOH during the longer leaching time. This change in the morphology indicates that Al had been removed from the alloy surface

during initial leaching leading to precipitation of Cu/Fe on the surface. Upon further leaching the Cu/Fe precipitates also react. The sizes of the precipitates are in the nano-meter range and bigger on the B2 surface compared to the QC surface.

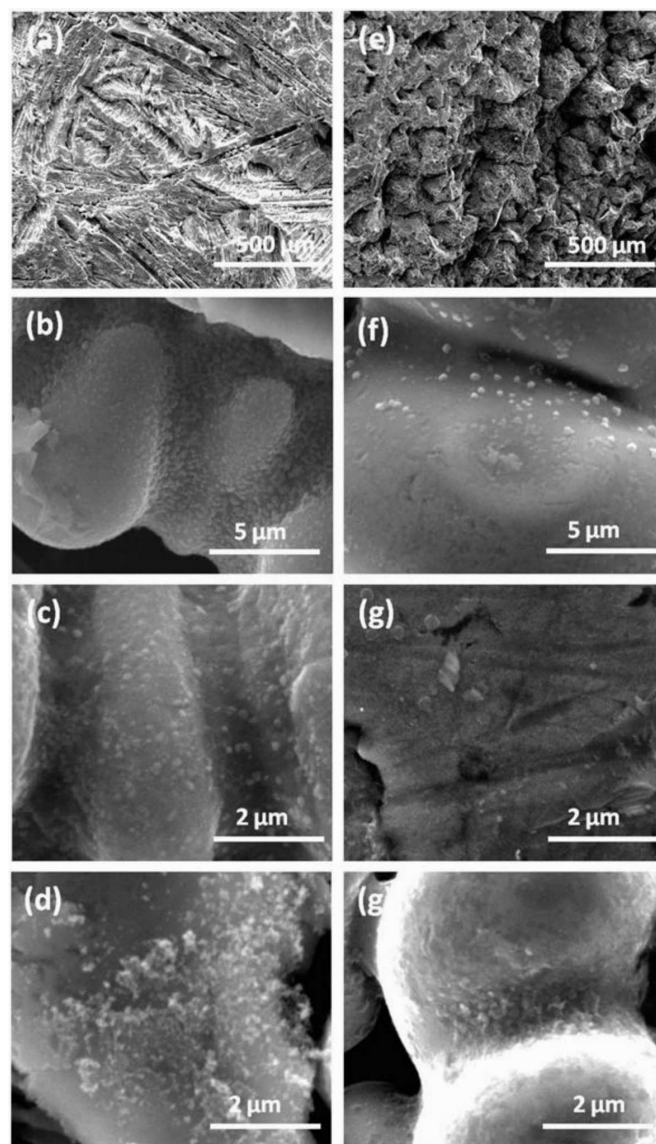


Fig. 1. SEM images of leached surface at different leaching time for (i)- $\text{Al}_{63}\text{Cu}_{25}\text{Fe}_{12}$ (a) 1 h, (b) 2 h, (c) 4 h, (d) 8 h and for (B2)- $\text{Al}_{55}\text{Cu}_{30}\text{Fe}_{15}$ (e) 1 h, (f) 2 h, (g) 4 h, (h) 8 h respectively.

Figure 2a and b shows XRD patterns of $\text{Al}_{63}\text{Cu}_{25}\text{Fe}_{12}$ quasicrystal annealed at $800\ ^\circ\text{C}$ for 10 h and subsequently leached in 10 mol NaOH aqueous solution at room temperature for 8 h (b). The X-ray diffraction peaks for the annealed sample can be assigned using the six-value index system proposed for the icosahedral phase allowing the identification of single quasicrystalline phase and indicating the homogeneity of the alloy. Extra diffraction peaks from Cu and Fe (Fig. 1b) are observed after leaching

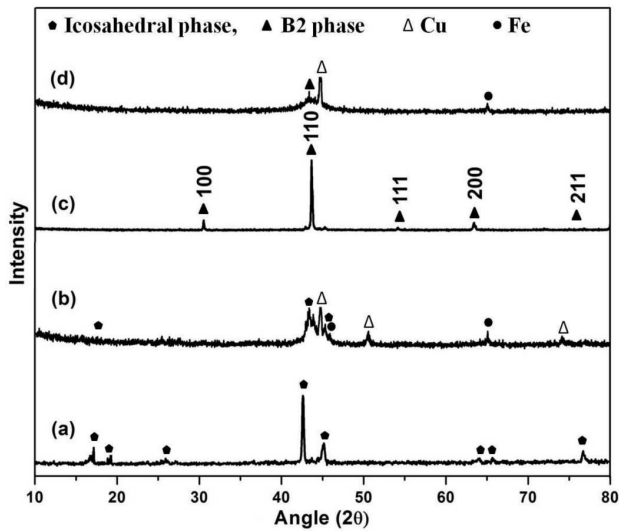


Fig. 2. (a) XRD patterns of the $\text{Al}_{63}\text{Cu}_{25}\text{Fe}_{12}$ quasicrystal annealed at 800°C for 10 h, and subsequently leached in 10 mol NaOH aqueous solution at room temperature for 8 h (b), (c) XRD patterns of the (B2)- $\text{Al}_{55}\text{Cu}_{30}\text{Fe}_{15}$ alloy obtained after annealing at 800°C for 10 h and subsequently leached in 10 mol NaOH aqueous solution at room temperature for 8 h (d).

treatment in NaOH solution. The use of the Voigt function for the analysis of the integral widths of broadened X-ray diffraction line profiles allows rapid determination of crystallite size and strain. The size of the Cu particles was found to be ≈ 12 nm based on line broadening of the XRD peaks [22]. Figure 2c and d shows the XRD patterns for the (B2)- $\text{Al}_{55}\text{Cu}_{30}\text{Fe}_{15}$ alloy obtained after annealing at 800°C for 10 h and subsequently leached in 10 mole NaOH aqueous solution at room temperature for 8 h. B2 phase obtained from the as-cast ingot material was indexed with lattice parameter $a = 2.91 \text{ \AA}$. It can be seen that after leaching treatment for 8 h, the (110) peak of the B2 phase becomes broader and an intense peak of Cu and Fe was observed (Fig. 2d). These effects may be attributed to the leaching effect and the precipitation of nanoparticles. The size of the Cu and Fe particles was found to be ≈ 16 nm based on the line broadening of the XRD peaks.

In order to explore the microstructure of all the samples, TEM studies of the as-cast as well as leached (*i*)- $\text{Al}_{63}\text{Cu}_{25}\text{Fe}_{12}$ and (B2)- $\text{Al}_{55}\text{Cu}_{30}\text{Fe}_{15}$ alloys were carried out. Figure 3 shows representative microstructure of the 8 h leached (*i*)- $\text{Al}_{63}\text{Cu}_{25}\text{Fe}_{12}$ alloy. Nano-size grains can be seen in the microstructure around equiaxed grains of micron size (region *i*). The electron diffraction pattern taken from the region labelled *i* shows a QC pattern along a twofold axis, typically observed in quasicrystals with icosahedral symmetry. The sharp diffraction spots arrayed in a non-periodic way indicate quasicrystalline structure (Fig. 3b). Electron diffraction from region *L* shows the presence of spotty rings due to nanograin microstruc-

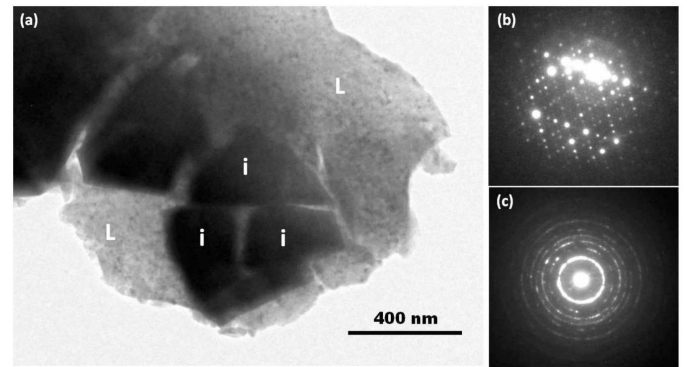


Fig. 3. (a) TEM microstructure of the 8 h leached (*i*)- $\text{Al}_{63}\text{Cu}_{25}\text{Fe}_{12}$ alloy, (b) SAD pattern taken from region *i* and (c) SAD pattern from region *L*.

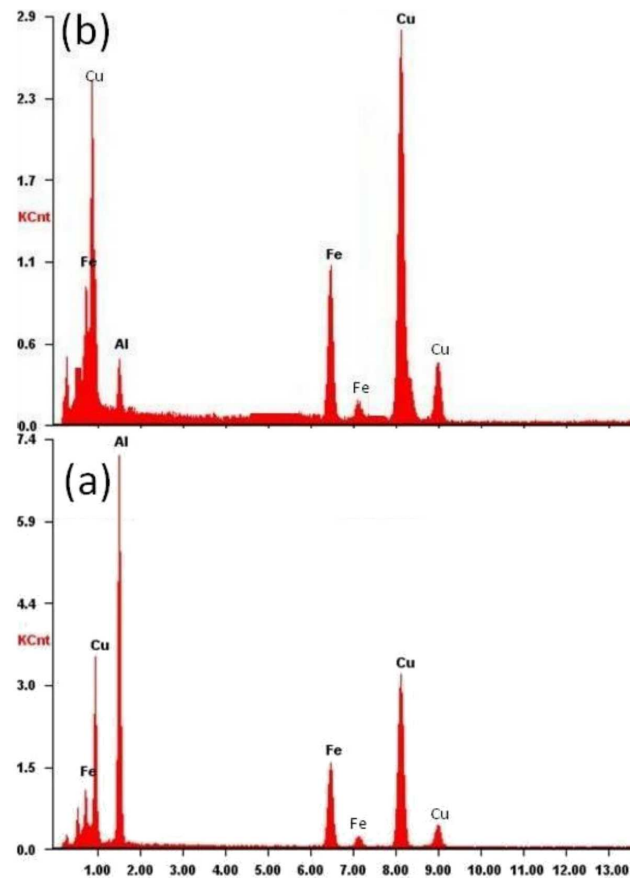


Fig. 4. The EDX spectra taken from both regions i.e. *i* (a) and *L* (b).

ture (Fig. 3c). This pattern has been commonly observed in all leached samples. EDX (Fig. 4) was taken from both regions (*i* and *L*) which confirms that Cu is 25 at.% and Fe is 20 at.% from the *i*-region whereas the corresponding values are 60 at.% and 30 at.% from region *L*. This indicates that Al is dissolved during leaching and the proportion of Cu and Fe increases correspondingly.

At the beginning of the leaching process i.e. below 0.5 h, the dissolution of Al and precipitation of Cu and Fe is very slow; however, it increases after 1 h of leaching.

4. Conclusions

The leaching of polygrain (*i*)-Al₆₃Cu₂₅Fe₁₂ and (*B2*)-Al₅₅Cu₃₀Fe₁₅ surfaces have been carried out for different time i.e. 1–8 h with 10 mol NaOH aqueous solution. On the leached surface of the QC phase, nanoparticles of transition metals (Cu and Fe) were found. Results on the chemical composition measured by EDX analyses indicate a significant removal of Al. The catalytic properties of the leached surface require further investigation.

Acknowledgments

T.P.Y. thanks the Department of Science and Technology (DST) for BOYACAST fellowship during which period a part of the work was completed. The financial support received from DST and Ministry of New and Renewable Energy, India (Mission Mode Hydrogen Storage Project) is gratefully acknowledged.

References

- [1] D. Shechtman, I. Blech, D. Gratias, J.W. Cahn, *Phys. Rev. Lett.* **53**, 1951 (1984).
- [2] J.M. Dubois, *Isr. J. Chem.* **51**, 1168 (2011).
- [3] J. M. Dubois, *Useful Quasicrystals*, World Scientific, Singapore 2005.
- [4] U. Köster, H. Liebertz, W. Liu, *Mater. Sci. Eng. A* **181-182**, 777 (1994).
- [5] J.M. Dubois, P. Weinland, French patent No. 8810559 (1988).
- [6] T.P. Yadav, D. Singh, R.S. Tiwari, O.N. Srivastava, *Mat. Lett.* **80**, 5 (2012).
- [7] M. Sales, A. Merstallinger, P. Brunet, M.C. de Weerd, V. Khare, G. Traxler, J.M. Dubois, *Philos. Mag.* **86**, 965 (2006).
- [8] S. Kenzari, D. Bonina, J. M. Dubois, V. Fournée, *Mater. Des.* **35**, 691 (2012).
- [9] S.B. Biner, D.J. Sordelet, B.K. Lograsso, I.E. Anderson, US Patent No. 5851317 (1998).
- [10] A.P. Tsai, M. Yoshimura, *Appl. Catal. A* **214**, 237 (2001).
- [11] M. Yoshimura, A.P. Tsai, *J. Alloys Comp.* **342**, 451 (2002).
- [12] B. Phung Ngoc, C. Geantet, M. Aouine, G. Bergeret, S. Raffy, S. Marlin, *Int. J. Hydrog. Energy* **33**, 1000 (2008).
- [13] K. Nosaki, T. Masumoto, A. Inoue, T. Yamaguchi, United state Patent No. 5800638 (1998).
- [14] C. J. Jenks, P. A. Thiel, *J. Mol. Catal. A: Chem.* **131**, 301 (1998).
- [15] S. Kameoka, T. Tanabe, A.P. Tsai, *Catal. Today* **93-95**, 23 (2004).
- [16] A.P. Tsai, S. Kameoka, M. Terauchi, United state Patent No. 7592292B2 (2009).
- [17] A.P. Tsai, S. Kameoka, M. Terauchi, European Patent No. EP 1666144A1 (2005).
- [18] T. Tanabe, S. Kameoka, A.P. Tsai, *Catal. Today* **111**, 153 (2006).
- [19] T. Tanabe, S. Kameoka, A.P. Tsai, *Appl. Catal. A: General* **384**, 241 (2010).
- [20] T. Tanabe, S. Kameoka, A. Tsai, *J. Mater. Sci.* **46**, 2242 (2011).
- [21] T.P. Yadav, M. Lowe, R. Tamura, R. McGrath, H.R. Sharma, *Aperiodic Crystals*, Eds.: S. Schmid, R.L. Withers, R. Lifshitz, Springer Science, 2013, p. 275.
- [22] T.P. Yadav, N.K. Mukhopadhyay, R.S. Tiwari, O.N. Srivastava, *Mat. Sci. Eng. A* **393**, 366 (2005).